Real-time energy market arbitrage via aerodynamic energy storage in wind farms

Carl R. Shapiro, Chengda Ji, and Dennice F. Gayme¹

Abstract—Energy storage can generate significant revenue by taking advantage of fluctuations in real-time energy market prices. In this paper, we investigate the real-time price arbitrage potential of aerodynamic energy storage in wind farms. This under-explored source of energy storage can be realized by deferring energy extraction by turbines toward the front of a farm for later extraction by downstream turbines. In large wind farms, this kinetic energy can be stored for minutes to tens of minutes, depending on the inter-turbine travel distance and the incoming wind speed. This storage mechanism requires minimal capital costs for implementation and potentially could provide additional revenue to wind farm operators. We demonstrate that the potential for revenue generation depends on the energy arbitrage (storage) efficiency and the wind travel time between turbines. We then characterize how price volatility and arbitrage efficiency affect real-time energy market revenue potential. Simulation results show that when price volatility is low, which is the historic norm, noticeably increased revenue is only achieved with high arbitrage efficiencies. However, as price volatility increases, which is expected in the future as the composition of the power system evolves, revenues increase by several percent.

I. INTRODUCTION

Electric power storage devices can generate considerable revenue through energy market arbitrage, where the storage operator buys and stores electricity at low prices and sells at a higher price [1]. In New York, battery storage devices were found to generate a median net revenue of \$50 per MW of capacity per day by arbitraging energy prices over 2 hour intervals [2]. Similar revenue potential was found for pumped hydro storage in Great Britain, however the revenue did not justify the large capital cost of these systems [3]. Energy arbitrage with distributed energy resources, such as electric vehicles [4] and electric water heaters [5], and through demand-response programs in buildings [6] has also been shown to be cost-effective. The price volatility that enables this arbitrage is expected to increase as generation from renewable resources continues to expand [7], further raising the revenue potential of real-time energy market arbitrage.

The control design in [8] exploited an aerodynamic energy storage mechanism to enable a wind farm to efficiently provide the minute-scale ancillary service, secondary frequency regulation. This storage of kinetic energy in the wind farm flow field can be accomplished by reducing energy extraction at upstream turbines, thereby increasing the energy available to subsequent turbines. More specifically,

¹Carl R. Shapiro, Chengda Ji, and Dennice F. Gayme are with the Department of Mechanical Engineering, Johns Hopkins University, Baltimore, Maryland 21218, USA cshapir5@jhu.edu, chengdaji@jhu.edu, dennice@jhu.edu

as the wind travels through a turbine, the extraction of kinetic energy leads to a less energetic region downstream, known as the turbine wake [9]. Reducing energy extraction at an upstream turbine leads to a more energetic wake. As this wake travels downstream, the additional energy can be partially extracted by subsequent turbines. The energy storage duration is proportional to the minute scale interturbine wind travel time and the number of rows in the farm. Inter-turbine wind travel times at rated power range from 30 seconds to 2 minutes in typical farms, resulting in storage durations of minutes to tens of minutes in moderately sized wind farms. Therefore, the mechanism is potentially applicable to real-time energy market price arbitrage with clearing times of five-minutes or less.

In this paper, we develop an optimization framework for energy arbitrage in 5-minute real-time markets via aerodynamic energy storage in wind farms. The feasibility and efficiency of the aerodynamic energy storage mechanism is first studied using high-fidelity computational fluid mechanics simulations [10], [11]. We construct a simplified model to estimate the revenue potential of such an approach under different farm configurations and price volatility scenarios. This model uses a graph representation of a wind farm [12] that is informed by high-fidelity simulation data. The modelbased control algorithm is used to study the revenue potential of energy market arbitrage for a wind farm operating under historic price and wind speed data. We then further analyze the revenue potential of this approach under different price volatility scenarios, as measured by a proposed inter-period volatility index. Under low volatility, which is the historic norm, aerodynamic energy arbitrage increases revenue by less than one percent. In scenarios with higher volatility, which is expected in the future, revenue increases by several percent.

The remainder of this paper is organized as follows. In Section II we demonstrate the aerodynamic energy storage potential of wind farms using high-fidelity simulations. We introduce a directed graph model of the wind farm and formulate the energy market arbitrage problem in Section III. In Section IV, we show energy market revenue results from simulations of the wind farm model. Finally, the implications of the results are discussed and conclusions are made in Section V.

II. AERODYNAMIC ENERGY STORAGE

Aerodynamic energy storage with wind farms has not been widely studied. In this section, we explain the aerodynamic storage mechanism using control actuation of the first row of turbines as an example. This actuation reduces power generation for a specified time period and results in additional power generation for the entire farm during a later time period by increasing power generation at downstream turbines. We then estimate the aerodynamic storage efficiency from high fidelity simulations of staggered and aligned wind farms operating at constant power coefficients.

To demonstrate the feasibility of aerodynamic energy storage for energy arbitrage, we consider a wind farm composed of 84 turbines arranged in 7 rows of 12 aligned columns. Rows and columns are defined as shown in Figure 2. The turbines are numbered as shown in Figure 3. Each turbine has a D=2R=100 m rotor diameter and a 100 m hub height. The spacing between turbines is $s_x=7D$ in the streamwise (aligned with the wind) direction and $s_y=5D$ in the spanwise (perpendicular to the wind) direction.

We assume idealized Betz-optimal wind turbines and neglect dynamic effects in turbine rotation rate and pitching actuation. With these assumptions, the power generation at the maximum power point of the i-th turbine is given by

$$P_i^{\text{max}} = \begin{cases} \frac{1}{2} \rho \pi R^2 C_P u_{\infty,i}^3 & u_{\infty,i} < u_{\text{rated}} \\ P_{\text{rated}} & u_{\text{rated}} < u_{\infty,i} < u_{\text{max}} \\ 0 & u_{\infty,i} > u_{\text{max}}, \end{cases}$$
(1)

where $u_{\infty,i}$ is the incoming wind speed to the *i*-th turbine, $u_{\rm rated}$ is the rated wind speed of the turbine, $u_{\rm max}$ is the cut-out wind speed of the turbine, and ρ is the air density. The rated power is $P_{\rm rated} = \frac{1}{2} \rho_0 \pi R^2 C_P u_{\rm rated}^3$, where $\rho_0 = 1.223 \text{ kg/m}^3$ is the nominal density of air. For the unwaked turbines, the inflow velocity is equal to the wind speed at the beginning of the farm $U_{\infty}(t)$.

This wind farm is simulated using high-fidelity computational fluid mechanics code that simulates the wind turbine array velocity field and the energy extraction by individual turbines. More information about the simulation environment can be found in [13], [14]. The power generation of the first row of turbines is modulated dynamically by controlling the power coefficient C_P to provide energy storage over a minute time scale. In particular, the power coefficient is adjusted such that the first row of turbines is turned off $C_{P,i}(t) = 0.5625 \left[1 - H(t+\tau) + H(t)\right], i = 1, \dots, 12$ for

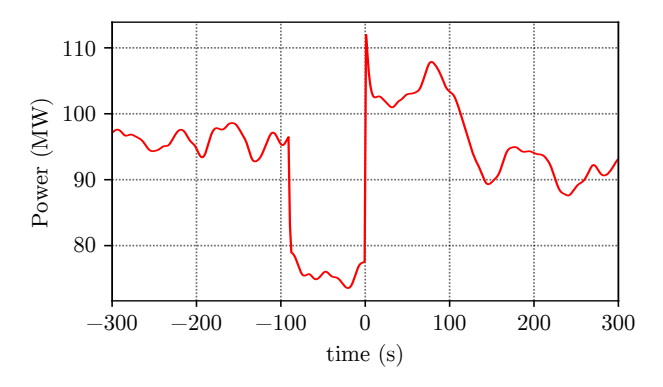


Fig. 1: Wind farm power when the first row turbines are turned off at t = -90 s and back on at t = 0.

 $\tau = 90$ s, where H(t) is the Heaviside function and all other turbines operate at $C_{P,i} = 0.5625, i = 13, \dots, N$.

The total power of this dynamically controlled wind farm is shown in Figure 1. Initially, all turbines are operating at $C_P = 0.5625$, generating approximately $P_0 = 96$ MW. At t = -90 s, the first row of turbines are turned off, $C_P = 0$, reducing the generation to approximately $P_{-} = 76 \text{ MW}$ and eliminating the wake behind the first row of turbines. After 90 seconds, which is the travel time between the turbine rows, the wake from the first row is no longer affecting the generation of the second row. At this point, the first row of turbines is turned back on, which increases the total wind farm power generation to approximately $P_{+} = 105$ MW. This increased generation continues until around t = 90 s, at which point the generation returns to approximately 96 MW. This experiment demonstrates that energy arbitrage through aerodynamic energy storage is feasible, and in this case the storage efficiency can be computed as $\alpha = (P_+ - P_0)/(P_0 - P_-) = 45\%$.

The instantaneous starting and stopping of wind turbines in this numerical experiment is unrealistic. However, these results provide an estimate of the efficiency of aerodynamic energy storage. Similar efficiencies with somewhat lower storage capacities can likely be obtained by pitch and torque control actuation over a few seconds.

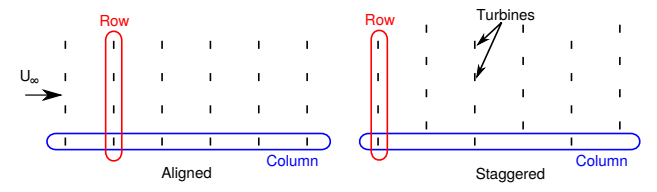


Fig. 2: Aligned and staggered wind farms with rows and columns shown. The direction of the wind velocity U_{∞} is also shown at the inlet to the aligned farm. Adapted from [8].

Storage efficiency in aligned farms can also be estimated from time-averaged power data of wind farms in aligned and staggered arrangements, as shown in Figure 2 [10]. Let P_1^a , P_2^a , and P_3^a denote the power production of the first three rows of an aligned wind farm under normal operating conditions, and P_1^s , P_2^s , and P_3^s denote the same quantities for a staggered wind farm. First, consider the power storage efficiency of the first row of turbines in an aligned farm. Turning off the first row of turbines reduces the power production of the farm by P_1^a . Once the wind travels to the second row, which produces P_2^a under normal waked conditions, the second row's power will increase to the first row's unwaked power generation P_1^a . The corresponding extra generation will be $(P_1^a - P_2^a)$ with a storage efficiency of $\alpha = (P_1^a - P_2^a)/P_1^a$. Energy can also be stored by reducing the generation of the second row. Consider the aligned wind farm in Figure 2. If the second row is turned off, then the third turbine will not be affected by the turbine's wake and will behave like the third row of turbines in the staggered wind farm in Figure 2. In this case, the inter-turbine distance will be doubled and the third row's power will increase from P_3^a to the power generated by the third row in a staggered farm P_3^s . The storage efficiency is then $\alpha = (P_3^s - P_3^a)/P_2^a$.

TABLE I: Aerodynamic energy storage efficiency when controlling rows 1 and 2 at various streamwise spacings s_x . Efficiencies calculated from data in [10].

s_x/D	Row 1	Row 2
7.85	0.44	0.43
5.24	0.59	0.53
3.49	0.72	0.76

Some example storage efficiencies for different streamwise inter-turbine spacings computed based on the simulation data in [10] are shown in Table I for various streamwise spacings s_x . The results are consistent with the storage efficiency found from simulations with dynamic modulation of the first row's power extraction. The storage efficiency decreases with increasing streamwise spacing and appears to be nearly constant regardless of the row that is controlled. The constant nature of the arbitrage efficiency for a given arrangement will form the basis of the wind farm price arbitrage model discussed in the next section.

III. PROBLEM FORMULATION

Consider a wind farm represented by a directed graph $\mathcal{G} = \{\mathcal{N}, \mathcal{E}\}\$, where the nodes $i \in \mathcal{N}$ represent the turbines and the edges $e_{ij} \in \mathcal{E}$ describe the interconnection of turbines through wake effects. The edges can be described by an adjacency matrix with $e_{ij} = 1$ if turbine i's wake affects turbine j and $e_{ij} = 0$ if turbine j cannot be affected by the wake of turbine i. Each edge is assigned an edge weight $\alpha(e_{ij})$ that represents the storage efficiency between connected turbines. In other words, $\alpha(e_{ij})$ is the fraction of any energy stored by turbine i that can be extracted by turbine j. Although the aerodynamics of wind turbines and farms is highly nonlinear, this assumption appears to hold for the present analysis based on the results in Section II. Each edge is also assigned a time-varying edge time delay $T_d(e_{ij},t)$ that represents the inter-turbine wake travel time between turbines i and j.

In this paper, we limit the configurations to aligned wind farms with regular streamwise spacings between turbines s_x (see Figure 2). In this configuration, the wind farm graph is simply a collection of directed line graphs, as shown in Figure 3. The results of the high-fidelity simulation based computations in Section II demonstrate that the inter-turbine storage efficiency α in these farm configurations is nearly constant across all of the wind farm edge connections. We therefore set the edge weights $\alpha(e_{ij}) = \alpha, \forall e_{ij} \in \mathcal{E}$ to a constant value. The corresponding time-delay between turbines i and j connected by edge e_{ij} ,

$$T_d(e_{ij}, t) = \frac{s_x}{U_{\infty}(t)},\tag{3}$$

is computed by assuming that the wakes travel at the inflow velocity $U_{\infty}(t)$ to the wind farm. This linear advection assumption has been previously used in dynamic wind farm models with good results [8], [15].

The maximum power generation at each turbine is given by (1), which requires knowledge of the incoming wind velocity to each turbine $u_{\infty,i}(t)$. For the set of unwaked turbines \mathcal{U} (i.e. the first row), the incoming wind speed to the turbine modeled as the average wind speed at the inlet to the farm $u_{\infty,i}(t) = U_{\infty}(t) \, \forall i \in \mathcal{U}$. For the set of downstream (waked) turbines $\mathcal{W} = \mathcal{N} \setminus \mathcal{U}$, the wind speed will be lower due to the effect of upstream turbine wakes. Further examination of simulation results [10] shows that the power generation of these turbines is nearly constant. We can therefore adopt the model that for a given arbitrage efficiency of an aligned wind farm α , the maximum power of waked wind turbines is a fraction $\beta = (1 - \alpha)$ of the unwaked turbines' maximum power. The corresponding inflow wind speed is $u_{\infty,i}(t) = U_{\infty}(t)\beta^{1/3}, \, \forall i \in \mathcal{W}$.

We formulate the problem of providing real-time energy market arbitrage with wind farms as the optimization problem (2). The objective function (2a) represents the wind farm operator revenue revenue and $\lambda(t)$ denotes the real-time locational marginal price (LMP) at the wind farm interconnection at time t, $P_i(t)$ is the power generation of the i-th turbine at time t, and δ_t is the time interval. In this formulation, we neglect subsidies like the production tax credit and renewable energy credits, which are expected to be phased out in the future. The power generation is upper bounded by the rated power of the turbine (2b) and the power available in the wind (2c)–(2d), which includes the maximum power point generation $P_i^{\rm max}$ and additional power stored in the wake through aerodynamic storage $P_{ij}^{\rm stored}$.

The stored power along the edge connecting j and l, $P_{jl}^{\rm stored}(t)$, is given in equation (2d), which measures the stored energy as the difference between the sum of the max power and the upstream power storage and the power $P_j(t)$ extracted by turbine j. The non-negative extracted power is subsequently upper-bounded by the sum of the maximum power and weighted upstream stored power (2b).

With these assumptions, we have constructed a wind farm representation that includes the dynamics of wind and wake travel. However, nonlinearities inherent in the aerodynamics of wind farms and the dynamics of wind turbine torque and pitch actuation have not been incorporated. Although changing wind directions are not considered here, this could be incorporated by making the graph topology time dependent. The simplifying assumptions applied here provide a realistic, yet tractable, formulation that can be used to evaluate the applicability of aerodynamic energy storage in real time energy markets. We next apply the approach described above to explore the revenue potential of real-time energy market arbitrage with aerodynamic energy storage through numerical examples.

IV. SIMULATIONS

The revenue generation potential of an 84-turbine wind farm, shown in Figure 3, is studied using the nodal real-time prices [16] for the Hudson Valley zone of the New York Independent System Operator (NYISO) on February 28, 2018. The five-minute real-time data is interpolated into

$$\max \sum_{t=1}^{T} \lambda(t) \sum_{i=1}^{N} \delta_t P_i(t), \tag{2a}$$

.t.
$$0 \le P_j(t) \le P_{\text{rated}},$$
 $\forall j \in \mathcal{N},$ (2b)

$$0 \le P_j(t) \le P_j^{\max}(t) + \sum_{e : i \in \mathcal{E}} \alpha(e_{ij}) P_{ij}^{\text{stored}}(t), \qquad \forall j \in \mathcal{N},$$
 (2c)

s.t.
$$0 \le P_{j}(t) \le P_{\text{rated}},$$
 $\forall j \in \mathcal{N},$ (2b)
 $0 \le P_{j}(t) \le P_{j}^{\text{max}}(t) + \sum_{e_{ij} \in \mathcal{E}} \alpha(e_{ij}) P_{ij}^{\text{stored}}(t),$ $\forall j \in \mathcal{N},$ (2c)
 $P_{jl}^{\text{stored}}(t + T_{d}(e_{jl})(t)) = P_{j}^{\text{max}}(t) + \sum_{e_{ij} \in \mathcal{E}} \alpha(e_{ij}) P_{i,j}^{\text{stored}}(t) - P_{j}(t),$ $\forall e_{jl} \in \mathcal{E}.$ (2d)

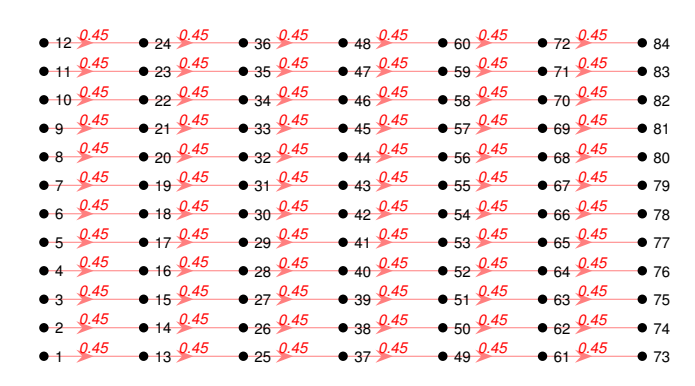


Fig. 3: Graph structures for an 84-turbine aligned wind farm with 7 rows, 12 columns, and $\alpha = 0.45$. Nodes are shown in black. Edges and edge weights are shown in red.

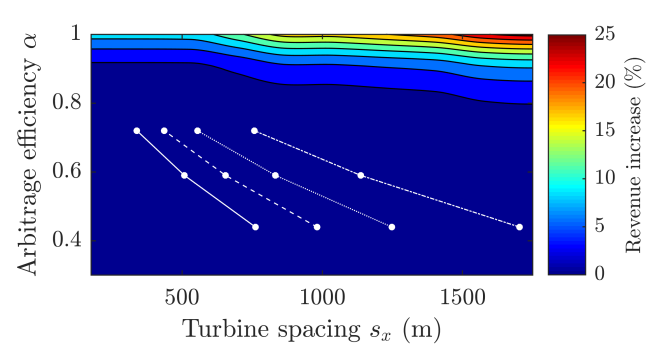


Fig. 4: Revenue increase under historical prices for various arbitrage efficiencies α and turbine spacing. Realistic arbitrage efficiencies and spacings are also shown (in white) for wind farms composed of turbines with power ratings of 3, 5, 8, and 15 MW.

minute data for the revenue maximization problem in (2). Historical wind speed data [17] for the same location and day is used to construct the maximum power point generation of the wind farm. We first conduct a parametric study by varying the arbitrage efficiency α and turbine spacing s_x , as shown in Figure 4.

As expected, revenue increases with greater turbine spacing. The revenue increase is strongly dependent on the arbitrage efficiency, increasing dramatically for $\alpha > 0.9$. In real wind farms, however, arbitrage efficiencies are limited by aerodynamics and strongly related to the inter-turbine

spacing, which typically ranges from three to seven rotor diameters, $s_x = 3D-7D$. Figure 4 superimposes the values associated with realistic turbine spacings and efficiencies corresponding to the configurations used in [10], for different wind turbine power ratings plotted over the parameter sweep in white. Greater turbine power ratings correspond to larger rotor sizes and turbine spacing. In all cases, the revenue increases are near or less than 1% for realistic configurations.

Price volatility is expected to increase as the composition of the power system evolves. To evaluate this situation we consider the revenue potential of aerodynamic energy storage under scenarios with varying price volatility. Synthetic realtime prices, $\lambda_{\gamma}(t) = \lambda_{l}(t)v(t)$, are generated by multiplying the historic prices λ_l by a random number v drawn from a beta distribution given by

$$p(v) = \frac{\Gamma(2\gamma)}{2\Gamma^2(\gamma)} v^{\gamma - 1} (1 - v)^{\gamma - 1}.$$
 (4)

Values of γ are selected ranging from 0 to 1.

A quantitative index is needed to evaluate the volatility of the prices generated in this manner, as standard definitions of price volatility, e.g., variance or price spread, may not be relevant to aerodynamic energy storage in wind farms. Therefore, we propose an inter-period volatility index, as a measurement of the arbitrage capacity of a LMP trajectory under no efficiency losses; i.e., the downstream turbines receive all un-extracted power. This inter-period volatility index,

$$\Psi = \left(1 - \overline{E_{\lambda}}\right),\tag{5}$$

is determined by the mean value of the price increase trajectory, which is denoted as E_{λ} and given by

$$E_{\lambda}(t) = \begin{cases} \exp\left(1 - \frac{\lambda(t+1)}{\lambda(t)}\right), & \text{if } \lambda(t) > 0 \ \& \ \frac{\lambda(t+1)}{\lambda(t)} > 1, \\ 0, & \text{if } \lambda(t) \leq 0 \ \& \ \lambda(t+1) > 0, \\ 1, & \text{otherwise}, \end{cases}$$

where $t \in \{1, \dots, T-1\}$, and T is the length of the LMP trajectory. $\Psi \in [0,1]$ is a nonegative parameter with larger values indicating greater arbitrage capacity. $\Psi = 1$ indicates that arbitrage occurs during all time intervals, whereas, $\Psi =$ 0 indicates that there is no arbitrage potential because the LMP trajectory either goes down or remains constant.

Some example LMP trajectories under three different inter-period volatility index scenarios are shown in Figure 5.

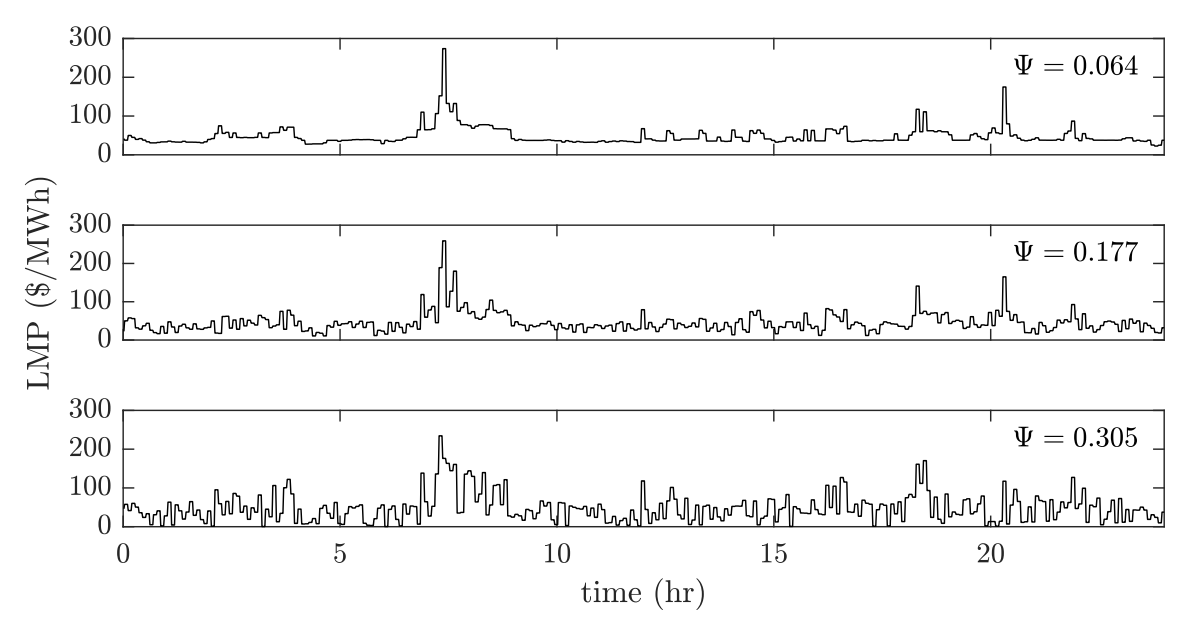


Fig. 5: LMPs under various inter-period volatility index scenarios.

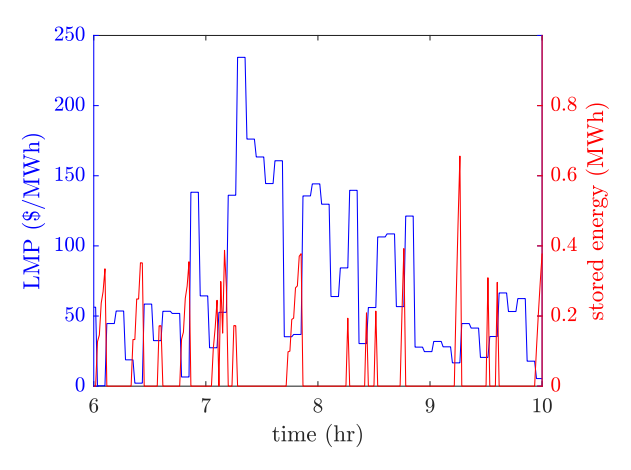


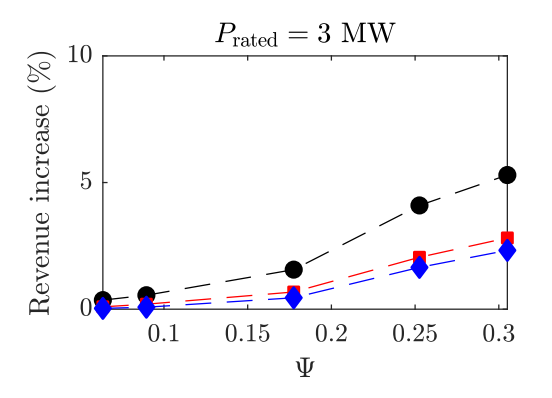
Fig. 6: LMPs and stored energy from 6am to 10am for 15 MW turbines spaced 3.49D apart.

Revenue increases as a function of the inter-period volatility index for wind farms with different wind turbine power ratings and turbine spacings are shown in Figure 7. Under a large inter-period volatility index, revenue potential increases substantially, reaching nearly 10% for 15 MW turbines reasonably closely spaced at 3.49D apart, which is about half of the typical inter-turbine spacing of installed farms. For this case, the energy storage from 6 am to 10 am is shown in Figure 6. As expected, energy is stored in advance of large relative price increases.

V. DISCUSSION AND CONCLUSIONS

This feasibility study of the revenue potential of real-time energy market arbitrage using aerodynamic energy storage in wind farms highlights the potential use of aerodynamic storage and the efficiency of this storage mechanism. The results of the simulations presented here indicate that historic price volatility in NYISO does not provide significant revenue increases for wind farms using aerodynamic energy storage for real-time energy market arbitrage. Under higher price volatility scenarios, however, wind farms can generate significantly increased revenue. This is particularly true for large, closely-spaced turbines. These two trends may simultaneously occur in the near future as increased renewable generation affects prices and wind farms composed of large turbines are built offshore. We believe these results and potential future changes in the power grid and wind power plants demonstrate that additional investigation of this approach is warranted. In particular, aerodynamic energy storage could potentially provide additional revenue to wind farm operators as the renewable energy market model evolves beyond "must-take" and production tax credits.

This work made several simplifying assumptions whose validity needs to be further studied to fully understand the potential of the proposed approach in practice. For example, we assumed perfect knowledge of wind farm power output and real-time energy LMP predictions. The fidelity of the results would be improved by incorporating existing prediction methods. Wind power predictions over 1-5 hour horizons are possible using persistence models or mass-spring damper models of the unsteady Ekman layer [18], [19]. Real-time LMP predictions based on historical prices, power demand, and weather data are also the topic of on-going research, e.g., [20]. Extensions of the work accounting for uncertainty in these price and wind speed predictions will provide an estimate of how tight of an upper bound the current results provide for revenue potential. Furthermore, detailed wind turbine control algorithms need to be developed to implement this approach, and refined wind farm models are needed to account for aerodynamic nonlinearities.



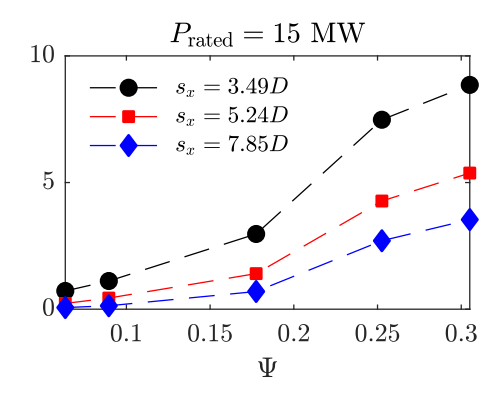


Fig. 7: Revenue increase versus the inter-period volatility index Ψ of LMPs under different price volatility scenarios and streamwise turbine spacings.

Coupling the aerodynamic storage mechanism discussed in this paper with other wind farm storage approaches could enhance the revenue potential of real-time energy market arbitrage with wind farms. For example, kinetic energy storage in the rotating rotor [21] could improve the storage efficiency. Such an approach has been previously used to reduce short-term fluctuations in power generation [21] and provide primary frequency regulation [22]. Aerodynamic storage could also increase the effectiveness of other storage mechanisms, such as co-located batteries [23]. As with all dynamic control applications, the effect of control actions on wind turbine loading and maintenance can be considerable and will affect the total profits of wind farms using aerodynamic energy arbitrage. These considerations are directions of ongoing work.

ACKNOWLEDGEMENTS

The authors acknowledge funding from the National Science Foundation (grant numbers CMMI 1635430 and ECCS 1711188) and the U.S. Department of Energy (award number DE-EE0008006). Computations made possible by the Maryland Advanced Research Computing Center (MARCC). The authors thank Charles Meneveau, Ben Hobbs, and Enrique Mallada for their insightful conversations.

REFERENCES

- M. Salles, J. Huang, M. Aziz, and W. Hogan, "Potential arbitrage revenue of energy storage sys. in PJM," *Energies*, vol. 10, no. 8, p. 1100, 2017.
- [2] R. Walawalkar, J. Apt, and R. Mancini, "Economics of electric energy storage for energy arbitrage and regulation in New York," *Energy Policy*, vol. 35, no. 4, pp. 2558–2568, 2007.
- [3] E. Barbour, I. G. Wilson, J. Radcliffe, Y. Ding, and Y. Li, "A review of pumped hydro energy storage development in significant international electricity markets," *Renewable and Sustainable Energy Reviews*, vol. 61, pp. 421–432, 2016.
- [4] A. Schuller, B. Dietz, C. M. Flath, and C. Weinhardt, "Charging strategies for battery electric vehicles: Economic benchmark and v2g potential," *IEEE Trans. Power Sys.*, vol. 29, no. 5, pp. 2014–2022, 2014.
- [5] N. J. Cammardella, R. W. Moye, Y. Chen, and S. P. Meyn, "An energy storage cost comparison: Li-ion batteries vs distributed load control," in 2018 Clemson University Power Sys. Conf. IEEE, Sep 2018.
- [6] J. L. Mathieu, M. Kamgarpour, J. Lygeros, and D. S. Callaway, "Energy arbitrage with thermostatically controlled loads," in *European Crtl. Conf.*, Zurich, Switzerland, July 2013, pp. 3120–3131.

- [7] J. C. Ketterer, "The impact of wind power generation on the electricity price in germany," *Energy Economics*, vol. 44, pp. 270–280, 2014.
- [8] C. R. Shapiro, P. Bauweraerts, J. Meyers, C. Meneveau, and D. F. Gayme, "Model-based receding horizon control of wind farms for secondary frequency regulation," Wind Energy, vol. 20, no. 7, pp. 1261–1275, 2017.
- [9] R. J. Barthelmie, K. Hansen, S. T. Frandsen, O. Rathmann, J. G. Schepers, W. Schlez, J. Phillips, K. Rados, A. Zervos, E. S. Politis, and P. K. Chaviaropoulos, "Modelling and measuring flow and wind turbine wakes in large wind farms offshore," *Wind Energy*, vol. 12, no. 5, pp. 431–444, 2009.
- [10] R. J. Stevens, D. F. Gayme, and C. Meneveau, "Effects of turbine spacing on the power output of extended wind-farms," Wind Energy, vol. 19, no. 2, pp. 359–370, 2016.
- [11] B. Sanderse, S. Pijl, and B. Koren, "Review of computational fluid dynamics for wind turbine wake aerodynamics," *Wind Energy*, vol. 14, no. 7, pp. 799–819, 2011.
- [12] J. Annoni, C. Bay, T. Taylor, L. Pao, P. Fleming, and K. Johnson, "Efficient optimization of large wind farms for real-time control," in *American Crtl. Conf.*, Milwaukee, WI, 2018, pp. 6200–6205.
- [13] R. J. A. M. Stevens, L. A. Martínez, and C. Meneveau, "Comparison of wind farm large eddy simulations using actuator disk and actuator line models with wind tunnel experiments," *Renew. Energy*, vol. 116, no. Part A, pp. 470 – 478.
- [14] "LESGO: A parallel pseudo-spectral large-eddy simulation code," https://lesgo.me.jhu.edu, 2019.
- [15] C. R. Shapiro, G. M. Starke, C. Meneveau, and D. F. Gayme, "A wake modeling paradigm for wind farm design and control," *Energies*, vol. 12, no. 15, p. 2956, 2019.
- [16] New York Independent System Operator, internet:http://www.nysio.com.
- [17] C. Draxl, A. Clifton, B.-M. Hodge, and J. McCaa, "The wind integration national dataset (WIND) toolkit," *Applied Energy*, vol. 151, pp. 355–366, 2015.
- [18] M. Momen and E. Bou-Zeid, "Large-eddy simulations and damped-oscillator models of the unsteady ekman boundary layer," *Journal of the Atmospheric Sciences*, vol. 73, no. 1, pp. 25–40, 2016.
- [19] E. Bou-Zeid and M. Momen, "System and method for performing wind forecasting," U.S. Patent 20180062393A, 2018.
- [20] Li Zhang and P. B. Luh, "Neural network-based market clearing price prediction and confidence interval estimation with an improved extended Kalman filter method," *IEEE Trans. Power Sys.*, vol. 20, no. 1, pp. 59–66, Feb 2005.
- [21] S. De Rijcke, J. Driesen, and J. Meyers, "Power smoothing in large wind farms using optimal control of rotating kinetic energy reserves," *Wind Energy*, vol. 18, no. 10, pp. 1777–1791, 2015.
- [22] J. Aho, A. Buckspan, J. Laks, P. Fleming, Y. Jeong, F. Dunne, M. Churchfield, L. Pao, and K. Johnson, "A tutorial of wind turbine control for supporting grid frequency through active power control," in *American Crtl. Conf.*, Montreal, QB, June 2012, pp. 3120–3131.
- [23] S. Teleke, M. Baran, A. Huang, S. Bhattacharya, and L. Anderson, "Control strategies for battery energy storage for wind farm dispatching," *IEEE Trans. Energy Conversion*, vol. 24, no. 3, pp. 725–732, 2009.